Joule

CellPress

Article

The sensitivity of power system expansion models

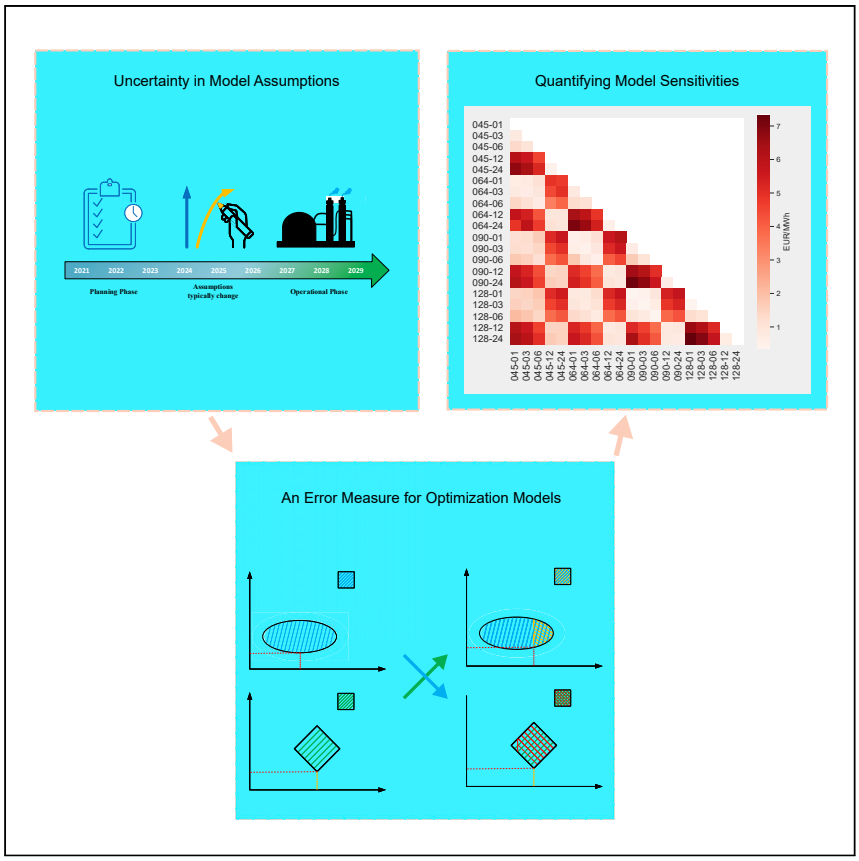

Optimization models are a widely used tool in academia. They come with their own weaknesses and uncertainties. Here, we show that the sensitivity of optimization models can systematically be described by quantifying the error originating from uncertain model parameters and model designs. Using the example of power system models, we emphasize that disclosing sensitivity information can contribute to openness and transparency in research. Power system optimization models are found to be especially sensitive to the temporal resolution.

Bruno U. Schyska, Alexander Kies, Markus Schlott, Lueder von Bremen, Wided Medjroubi

bruno.schyska@dlr.de

Highlights

An error metric allows to quantify optimization model sensitivities

The metric can be applied to both, model parameters and model designs

Encourages to disclose sensitivity information together with the model results

Power system models are particularly sensitive to the temporal resolution

Schyska et al., Joule 5, 2606–2624
October 20, 2021
https://doi.org/10.1016/j.joule.2021.07.017

CellPress

Joule

Article

The sensitivity of power system expansion models

Bruno U. Schyska,[1,3,*] Alexander Kies,[2] Markus Schlott,[2] Lueder von Bremen,[1] and Wided Medjroubi[1]

SUMMARY

Optimization models are a widely used tool in academia. In order to build these models, various parameters need to be specified, and often, simplifications are necessary to ensure the tractability of the models; both of which introduce uncertainty about the model results. However, a widely accepted way to quantify how these uncertainties propagate does not exist. Using the example of power system expansion modeling, we show that uncertainty propagation in optimization models can systematically be described by quantifying the sensitivity to different model parameters and model designs. We quantify the sensitivity based on a misallocation measure with clearly defined mathematical properties for two prominent examples: the cost of capital and different model resolutions. When used to disclose sensitivity information in power system studies our approach can contribute to openness and transparency in power system research. It is found that power system models are particularly sensitive to the temporal resolution of the underlying time series.

INTRODUCTION

In order to address the issue of climate change and sustainability, countries around the world make great efforts to transform their energy systems. In this context, large shares of weather-dependent renewable power sources need to be integrated into existing power systems.[1] This is a challenging task and requires a great number of political decisions. The societal and political decision-making process is accompanied by energy system research, which proposed manifold approaches to support the integration of renewable resources.[2,3] These approaches include the large-scale integration of storage technologies,[4,5] the extension of the transmission grid,[6,7] the over-installation of renewable capacities,[8] the use of meteorological information to find the optimal spatial deployment,[9] or optimizing the mix of different renewable generation sources.[10–12] The question whether resources such as nuclear or fossil power plants with carbon capture and storage can help achieve the decarbonization of the power system has recently been addressed by Sepulveda et al.[13] and Brown and Botterund[14] (among others). Kies et al.[15] found that demand-side management can balance generation-side fluctuations for a renewable share of up to 65% in Europe. Hirth and Muller,[16] Chattopadhyay et al.,[17] and Pfenninger et al.[18] proposed to deploy system-friendly generation assets. Lund and Kempton[19] proved the usefulness of vehicle-to-grid technologies for the integration of renewables, and Brown et al.[20] investigated the synergies between the sectors electricity, heat, and transportation.

Many of these solutions are the result of studies using power system expansion models (PSEMs). In most cases, studies using PSEMs have the aim to find the least expensive design of a power system given the constraint that the CO_2 emissions from power plants may not exceed an upper limit. They are used not only in research

Context & scale

Power system models are a widely used tool in academia. They support the societal and political decision-making process in the context of the transformation of power systems. In particular, they can propose approaches to ease the integration of renewable resources. However, model results are subject to uncertainties originating from uncertain model parameters or model formulations.

Here, we show that the error caused by uncertain assumptions for model parameters or model designs can be measured by a mathematically well-defined concept: a distance measure (or metric). When applied in a systematic manner, this metric can be used to describe the sensitivity of many kinds of optimization models. Therefore, it is found that power system models are especially sensitive to the temporal resolution. We emphasize that our approach could be used as a standard to disclose sensitivity information in power system studies and, hence, contribute to openness and transparency.

but also for policy advise and as a basis for far-reaching political decisions and societal discussions.[21–23] Considering the potential outreach of the results, the models and assumptions behind them should be trustworthy and transparent.[24]

Mathematically, PSEMs are often expressed as a linear program (LP) of the general form:

$$\min_x \quad c^T x \qquad \text{(Equation 1)}$$

$$\text{s.t} \quad Ax \geq b$$

$$x \geq 0$$

PSEMs combine several aspects being described by a set of socio-economical, technical, and meteorological parameters. Model formulation and structure must be chosen in a way that ensures the tractability of the model and the ability to deal with long time series of load and meteorological data.[25,26] Together, model structure and the choice of the parameters define the coefficient matrix A, the vector b, and the objective coefficients *c* of the LP. They determine the actual problem: the dimensionality and shape of the solution space.[27] In turn, the choice of the parameters and the model structure determine the simulation results.[28–30] If *A* and/or *b* and/or *c* are modified, the solution of the LP changes depending on the model's sensitivity to the respective parameters and/or structure. Consequently, making good assumptions and reasonable choices for/of the model parameters and structure is of crucial importance. The uncertainty related to these choices leads to additional uncertainty related to the model results.[31–33] Having a deep understanding of this process appears fundamental to the public debate about the conversion of the power system.

Based on a global sensitivity analysis,[34] it was found that the uncertainty of economic parameters has the highest influence on the results of an energy model. Similarly, a study[35] investigated the robustness of a fully renewable power system model of France to uncertainties in the future cost of generation technologies. They found that although the optimal generation mix clearly depends on the respective cost for the different technologies, overall system costs are relatively insensitive. Recently, Nacken et al.[36] applied a method called modeling to generate alternatives[37–39] (MGA) to a future German energy supply and showed that it produces a number of significantly different energy scenarios. MGA is based on changing the PSEM structure by setting the cost-optimal objective value plus some slack as a new constraint and exploring the resulting solution space. Another study[27] used a similar method to explore the near-optimal solution space of a cost-optimized European power system. They observed a high variance in the deployment of individual components near the optimal solution. Another not directly related kind of uncertainty is introduced by the use of learning curves, which are commonly applied to account for cost reductions of certain technologies in pathway-optimizations.[40] The term learning curve refers to the concept according to which cumulative experience in the production of a product increases efficiency in the use of inputs and leads to cost reductions. These learning curves are typically non-linear and introduce non-convexities to the solution space, which are hard to resolve.[41] A graphical depiction of this effect is shown in Figure 1. For an overview of methods applied in the context of uncertainty in power system modeling, see Yue et al.[42]

The aim of this paper is the concise description of the implications of uncertainties on the results of PSEMs. We do this by analyzing the sensitivity of a common power system expansion model to different model parameters and structures based on a

[1]German Aerospace Center (DLR), Institute of Networked Energy Systems, Oldenburg, Germany

[2]Frankfurt Institute for Advanced Studies, Goethe University, Frankfurt, Germany

[3]Lead contact

*Correspondence: bruno.schyska@dlr.de

https://doi.org/10.1016/j.joule.2021.07.017

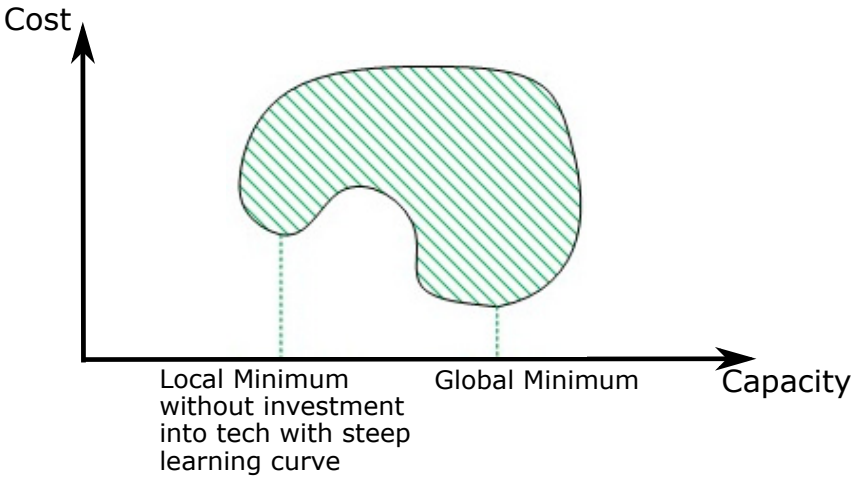

Figure 1. Learning curves introduce additional uncertainty

Schematic representation of non-convexities caused by learning curves. If a solver starts in the left part, it might run into the local optimum, whereas investments into the technology reduce cost in the medium-term and lead to the global optimum.

metric, which expresses the error of PSEM results when deciding for one of two plausible assumptions (in the following referred to as *scenarios*) α_i and α_j as the increase in the objective function values Γ:

$$M_{\alpha_j}^{\alpha_i} = \frac{[\Delta\Gamma]^{\alpha_i} + [\Delta\Gamma]^{\alpha_j}}{2} \quad \text{(Equation 2)}$$

Commonly, model parameters are derived from a collection of different data sources. The background of the approach introduced here is that the assumptions made for setting up a model, which shall be used to make decisions, are based on data observed at a different time from when the power system is planned. Meaning that planning and operation phase of energy system components are typically separated by long times, during which assumptions or knowledge can dramatically change (see Figure 2). Here, we assume that planning and operation phase can be expressed by two different scenarios α_i and α_j. However, this approach can easily be generalized to measure the sensitivity of linear programs to any assumptions made about model parameters and/or the model structure. It allows to cross-validate input data and to find representative datasets. By exemplarily quantifying the sensitivity of a simple PSEM to the definition of the cost of capital (as an example for model parameters) as well as to the spatial and temporal resolution of the model (as an example for the model structure), this study introduces a standardized way to disclose the uncertainties of power system studies and, hence, contributes to increasing transparency in power system research.

RESULTS

The sensitivity to the cost of capital—an introductory example

In the formulation used here, the PSEM (1) consists of two problems (also referred to as levels). While the design problem minimizes the investment cost in generation, storage, and transmission capacities keeping all capacities within given bounds, the operation problem minimizes the operational cost of the power system ensuring that electricity generation meets the demand and keeps the generation lower or equal to the capacities derived from the design problem. For volatile renewable resources—such as wind and solar PV—the available dispatchable capacity is

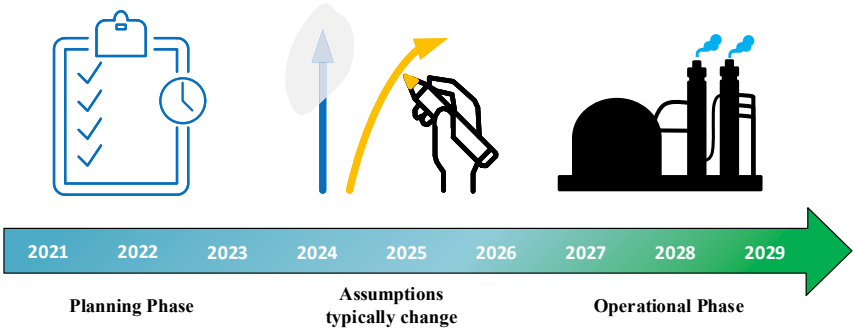

Figure 2. Planning and operation phase of energy system components are typically several years apart

Schematic representation of the original idea of our approach.

additionally limited by the prevailing meteorological conditions, i.e., the capacity factor time series. Furthermore, the consistency of the state of charge of storage units must be ensured.

Consequently, the capital costs for all generation, storage, and transmission assets are one of several major parameters to this PSEM, a subset of the objective coefficients c. These capital costs are influenced by the cost of capital, i.e., the costs an investor has to defray for his credits. It has been shown that for wind power projects, these costs of capital vary significantly between European countries.[43] Let us assume that we would like to investigate the error in the results of a simple PSEM originating from uncertainties in the definition of these costs of capital. In order to do this, we define two plausible realizations: the first scenario (hom) assumes a homogeneous (constant) distribution of the cost of capital across the European countries. The second scenario (dia) takes regional differences into account. The cost of capital is set as the weighted average cost of capital (WACC) reported from the diacore project.[43] In this scenario, the cost of capital is a function of the country. It ranges from 12% in the South-Eastern European Countries to only 4% in Germany (Figure 3).

The PSEM used for this example is the PyPSA-Eur model published by Hörsch et al.[44] in its "one-node-per-country" setup. It consists of one node per country in the European Union plus Norway, Switzerland, the United Kingdom, Croatia, Serbia, and Bosnia, and it includes time series of capacity factors for onshore and offshore—where applicable—wind power as well as solar PV power and time series of electricity demand for each substation. Furthermore, time series for the inflow into hydro reservoirs and run-off-river power plants and upper bounds for the extendable generation capacity per renewable technology and substation are included. Nodes are connected via simplified high-voltage direct current transmission links. A rather limited number of technologies is considered: wind (onshore + offshore), solar photovoltaics (PV), open-cycle gas turbines (OCGT), hydro (run-off-river, reservoirs, and pumped hydro), as well as large-scale battery and hydrogen storage units. Investment in these technologies and the operation are optimized over a year (2013) in hourly resolution assuming perfect foresight, inelastic demands, as well as limited allowance of transmission capacity expansion and CO_2 emissions. For further details, see power system model and data.

For the same setup, a study[29] has shown that the two scenarios hom and dia lead to significantly different solutions for the cost-optimal generation capacity layout x^*_{hom} and x^*_{dia}. In particular, the optimal solution for the dia scenario contains a larger share

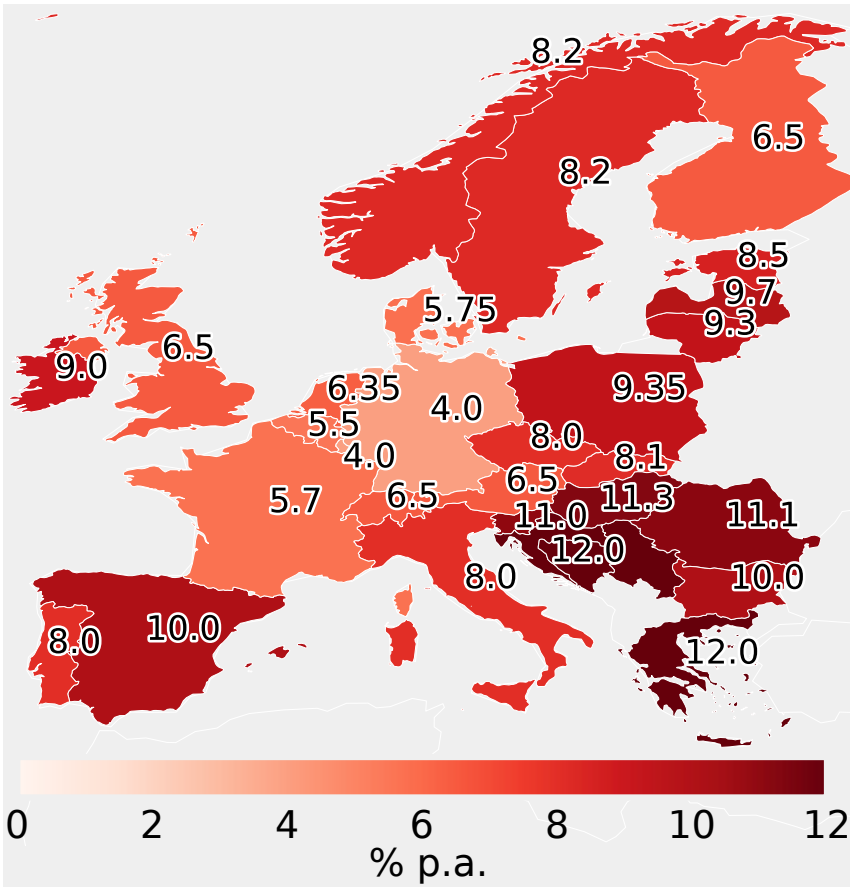

Figure 3. Inhomogeneous spatial distribution of the cost of capital
Weighted average cost of capital taken from Noothout et al.,[43] adopted from Schyska and Kies.[29]

of offshore wind power, whereas the shares of onshore wind power, solar photovoltaics (PV), and OCGT decrease compared with the hom scenario. However, the difference in the objective function values Γ_0^{hom} and Γ_0^{dia} is small (1.4 $\frac{EUR}{MWh}$, approximately 2% of the objective function values). Now, let us assume that one of the two scenarios shall be taken as the basis for the decision on where and how many large-scale PV farms should be erected. From the pure differences in x^* and Γ_0, one cannot tell with certainty whether this is a good decision or not. On the one hand, the error when deciding for one scenario might indeed be as large as the difference the optimal capacity layout x^* indicates. In this case, a great number of suboptimal investments would be made, leading to unnecessary high costs in the end, because the costs of capital, in reality, are different than the ones used for the planning. The difference in the objective function values would be small only by chance. On the other hand, the error might actually be small because the solution space is flat near the optimal point or a secondary optimum exists. Here, both solutions are almost equally valid. x^*_{hom} would solve the program from scenario *dia* at only little additional cost and vice versa. The decision to erect the PV farms either as proposed by the *hom* scenario or as proposed by the *dia* scenario is of minor importance.

In order to determine which of the two cases is true, one could set the solution x^*_{hom} as lower bound to the LP from scenario *dia* and vice versa, by adding the following constraints to each of the two models:

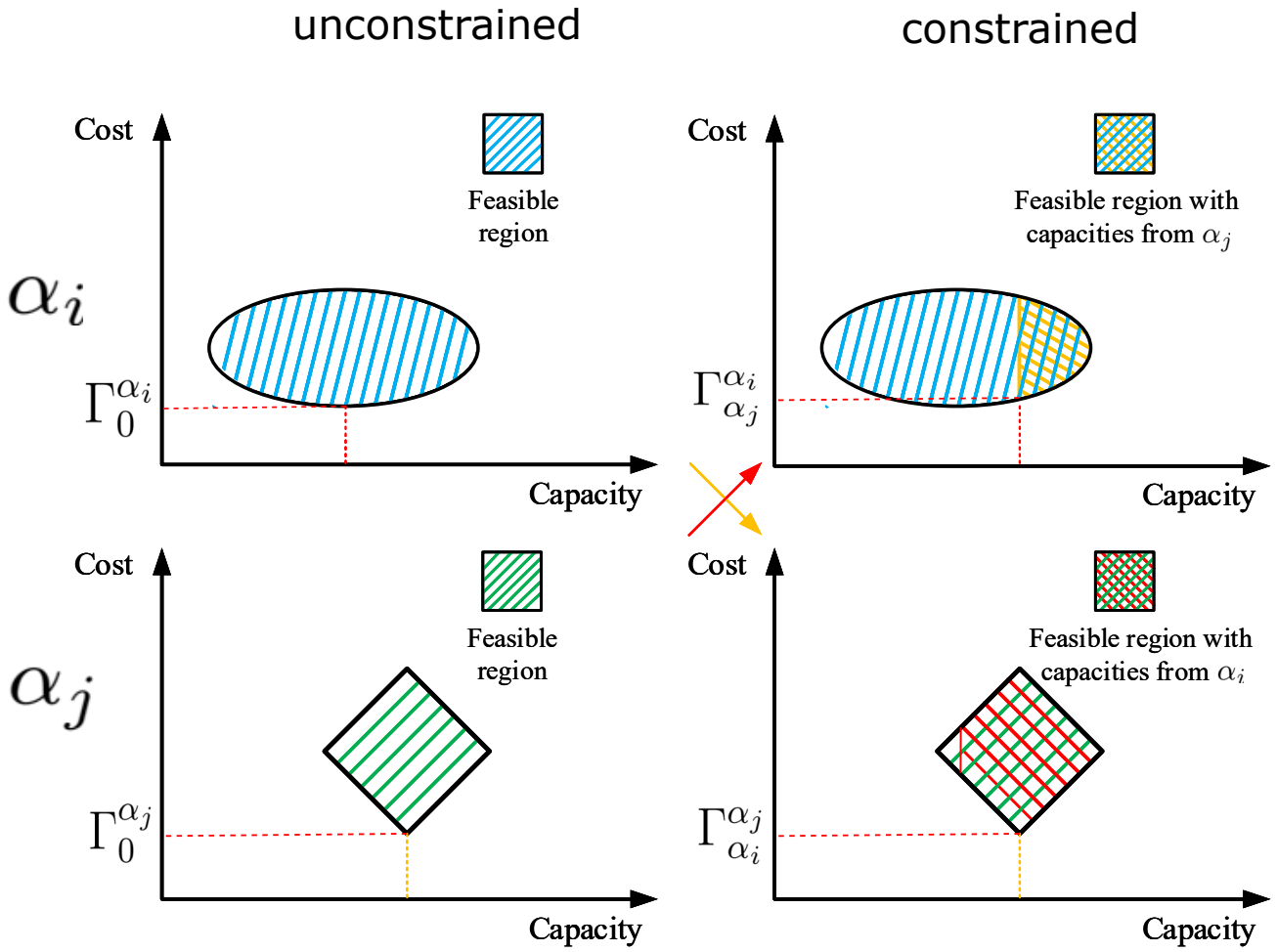

Figure 4. Measuring the error in optimization model results originating from uncertainties in model parameters and design

First, the original (unconstrained) problems using assumptions α_i and α_j are solved (left columns). Second, the solutions of these simulations are used for formulating additional constraints to the respective other problem (constrained problems, right column). The resulting differences in the cost $[\Delta\Gamma]^{\alpha_i} = \Gamma_{\alpha_j}^{\alpha_i} - \Gamma_0^{\alpha_i}$ can be used to measure the error. See text for further details.

$$x_{hom/dia} \geq x^*_{dia/hom} \qquad \text{(Equation 3)}$$

The program constructed, such as this, defines an upper bound to the original program. Hence, the optimal objective function value of that program is higher or equal to the objective function value of the original solution. If the second case is true, this rise in the objective function value, i.e., the levelized cost of electricity, should be small. However, invoking constraint (Equation 3) should cause a large additional cost in the first case. Then, the solution space is comparably steep, and/or x^*_{hom} is not a secondary optimum of the LP from scenario *dia*. Constraint (Equation 3) significantly messes up the optimization, leading to significantly higher costs. This cost increase can be measured via $[\Delta\Gamma]^{hom} = \Gamma^{hom}_{dia} - \Gamma^{hom}_0$, where Γ^{hom}_{dia} denotes the optimal value of the objective function with lower bounds defined by the optimal solution of the dia scenario. As one cannot tell which of the two scenarios is closer to reality (let us assume both scenarios are equally probable), this procedure should be performed in both directions (Figure 4). The potential error when deciding for one of the two scenarios can then be quantified as follows:

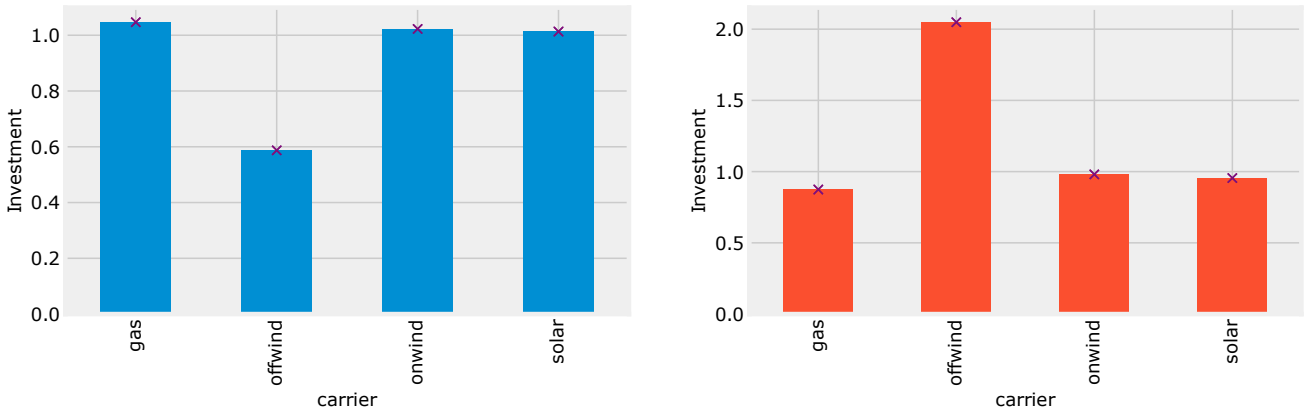

Figure 5. The spatial distribution of the cost of capital affects the cost-optimal investment

Investment in generation capacity relative to the unconstrained solution for the homogeneous scenario constrained with the solution of the diacore scenario (left, blue) and for the diacore scenario constrained with the solution of the homogeneous case (right, orange), crosses indicate the minimum investment for each generation source.

$$\begin{aligned} M_{dia}^{hom} &= \frac{[\Delta\Gamma]^{hom} + [\Delta\Gamma]^{dia}}{2} \\ &= \frac{1}{2}\left(\Gamma_{dia}^{hom} - \Gamma_{0}^{hom} + \Gamma_{hom}^{dia} - \Gamma_{0}^{dia}\right) \end{aligned} \qquad \text{(Equation 4)}$$

After computing Γ_{dia}^{hom} and Γ_{hom}^{dia}, one finds $M_{dia}^{hom} = 2.3\ \frac{EUR}{MWh}$. This is 3.3% (3.2%) of Γ_{0}^{hom} (Γ_{0}^{dia}). Recall that the difference in Γ_{0}^{hom} and Γ_{0}^{dia} suggests a smaller error of only 1.4 $\frac{EUR}{MWh}$. Here, we are able to show that the potential error indeed is higher than this difference.

This higher error can be explained by taking a look at the shape of the solution space: in general, the solution space for the design problem of the expansion problem is steeper than for the operation problems. This means that slight changes in the capacity layout may lead to significantly different investment cost, whereas there potentially exist many ways to solve the operational problem with similar cost. This effect is enhanced if additional regional differences in the cost of capital are considered. Building an offshore wind park in Germany or in Greece, for example, makes a bigger difference now as it made in the homogeneous case. For this example, we modified the regional distribution of the cost of capital cost but kept the nodal loads and the weather time series, which determine the availability of the volatile renewable resources, unchanged. Consequently, we find that both solutions of the unconstrained problems x_{dia}^{*} and x_{hom}^{*} also solve the operational problems of the respective other problem. All demands can be met with the prescribed capacities and no changes to the capacity layouts are necessary (Figure 5). However, since the two capacity layouts are quite different (as reported earlier) the investment cost in the constrained cases increases by 6% and 5%, respectively, compared with the unconstrained cases due to the different cost assumptions in the two scenarios (Figure 6).

Measuring the sensitivity of LPs to modifications of their model structure

A distinct strength of the proposed approach is that it can be used to measure the difference between the optimization results of any pair of LPs, which either (1) have the same decision variables, (2) have a common subset of decision variables, or (3) whose decision variables can be mapped on each other. Hence, it allows to systematically investigate the potential errors for a great number of scenarios. If all of these scenarios are related to the same aspect of the LP, this process can be

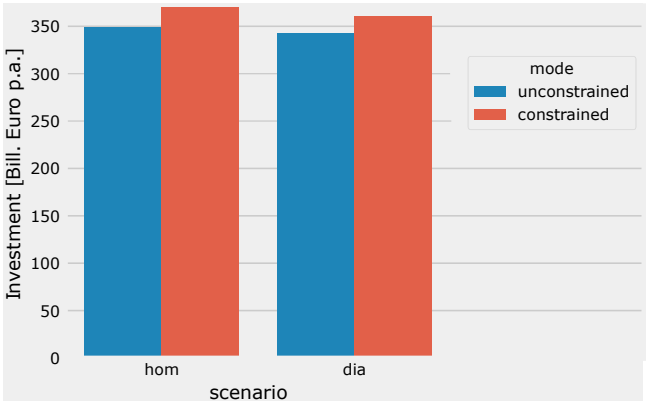

Figure 6. Investment costs increase due to different cost of capital

Investment for the two scenarios *hom* and *dia* in the unconstrained case (blue) and the constrained formulation (red).

understood as investigating the sensitivity of the considered program to modifications of that specific aspect. If errors are small overall, the sensitivity of the LP can also be considered small. The other way around, strong sensitivities should express themselves in large errors. As explained earlier, this not only applies to model parameters but also to the model structure, meaning that M can also measure the error (or the sensitivity) of a LP to changes in its own model structure. Here, we demonstrate this by investigating the sensitivity of the PyPSA-Eur[44] model (see the sensitivity to the cost of capital —– an introductory example and power system model and data) to modifications of its temporal and spatial resolution. In its full spatial and temporal resolution, PyPSA-Eur consists of 3,567 substations and 6,047 transmission lines and it covers 1 year in hourly resolution, i.e., 8,760 time steps. In this resolution, the PSEM can hardly be solved. In order to reduce the spatial resolution, the original network has been scaled down to 45, 64, 90, and 128 substations using the network clustering approach introduced by Hörsch and Brown.[45] The temporal resolution has been reduced by averaging the parameter time series over consecutive time spans of length $\tau \in \{3, 6, 12, 24\}$ h as described in reducing the spatial and temporal resolution of the model.

The sensitivity measure M for all possible combinations of these different resolutions (both spatial and temporal) exhibits a clear pattern (Figure 7). Basically, it can be divided into three different blocks: two blocks of (relatively) low sensitivity where $M \leq 4.2$ EUR/MWh and one of (relatively) high sensitivity where $M \geq 7.2$ EUR/MWh. The first block of low sensitivity contains all combinations of scenarios with a temporal resolution higher than 6 h, i.e., (*N*, 1H), (*N*, 3H), and (*N*, 6H), independent from the spatial resolution *N*. The second block of low sensitivity contains all combination of scenarios with a temporal resolution smaller than 12 h—again independent from the spatial resolution, and the block of high sensitivity contains all combinations of scenarios where one scenario has high ($\leq$ 6 h) temporal resolution and the other scenario has low temporal resolution ($\geq$ 12 h). From this definition of blocks, one can already see that the expansion problem is much less sensitive to changes in the spatial resolution as it is to changes in the temporal resolution. For instance, the sensitivity of the problem with hourly temporal resolution to increases in the spatial resolution from 45 nodes up to 128 nodes is below 4 EUR/MWh. In contrast, the sensitivity of the 128-node setup to reductions in the temporal resolution from hourly to minimum 12-hourly reaches a maximum value of almost 13 EUR/MWh.

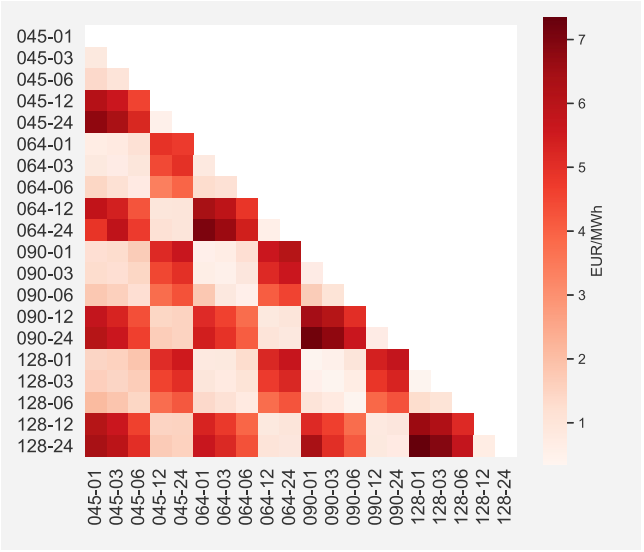

Figure 7. PSEM are particularly sensitive to the temporal resolution
Sensitivity heatmap [EUR/MWh]; in the tick labels, the number left of the hyphen indicates the number of nodes, the number right of the hyphen indicates the temporal resolution in hours.

The reasons for this are 2-fold. First of all, increasing the spatial resolution does not necessarily lead to a higher degree of information in the time series, and vice versa. Consequently, the results obtained from models with different spatial resolutions do not differ much. This phenomenon is of meteorological nature: hourly wind power and solar PV capacity factor time series exhibit large correlation lengths.[28,46] Consequently, aggregating nodes, which are geographically close, does not lead to a significant loss of information about the temporal characteristics of the aggregated nodes. For a detailed investigation of the correlation lengths of wind and solar PV in the PyPSA-Eur model see Section S1 in the supplemental information. In contrast, modifying the temporal resolution potentially leads to significant differences in the optimal capacity deployment, especially when the temporal resolution "jumps" from one of the blocks we defined earlier to another. The main reason for this is that downsampling the time series via averaging removes part of the temporal variability. In general, a rolling window averaging can be understood as a filter. For instance, averaging a time series with a rolling 24-h window filters out most of the sub-24 h variability of the time series, including the diurnal cycle (if present). If such a filter is applied to both the capacity factor time series and the demand time series, the residual load gets implicitly filtered as well. As a consequence, any storage technology meant to flatten the sub-12 h variability of the residual load time series would no longer be needed (because there is no sub-12 h variability).

In general, storage technologies can be assigned to a characteristic variability in the residual load time series via their energy-to-power ratio r, i.e., the number of hours they can store (dispatch) electricity at full power when starting from empty (full) storage. In the setup used here, batteries are characterized by an energy-to-power ratio of $r = 6$ h. They are meant to balance discrepancies between demand and availability, which occur on the intra-day scale. As described earlier, these discrepancies disappear when the demand and capacity factor time series are down sampled to a lower resolution. Consistently, no battery storage devices are optimally deployed in the model setups with a temporal resolution below 6 h (Figure 8). In contrast, hydrogen cavern storage units exhibit an energy-to-power ratio of $r = 168$ h, making

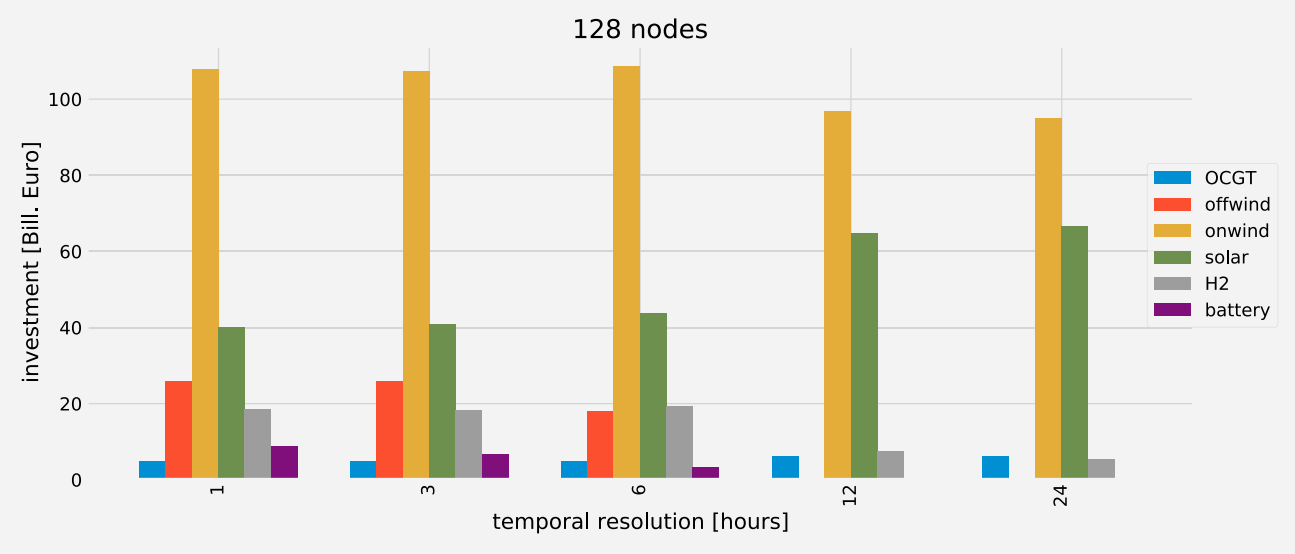

Figure 8. The temporal resolution affects the optimal deployment of storage capacities

Optimal investment in generation and storage capacity [billion Euro] for the 128-node network and for different temporal resolutions of the exogeneous parameter time series.

them a weekly storage. As the weekly variability is still present in the down-sampled time series, hydrogen storage devices are still useful.

In broad terms, filtering the high-frequency part of a time series' variability can be understood as removing scatter. This, in turn, also increases the correlation between the time series, again not only between the availability time series but also between the availability and the demand. Apparently, this rise in correlation mainly increases the system-friendliness of solar PV. Its investment share grows from approximately 40 billion Euro for the 3-hourly time series to more than 60 billion Euro for the 24-hourly time series (Figure 8). In turn, the importance of offshore wind power, which is mainly used to cover the baseload in the highly resolved model, decreases because the filtered time series no longer contain any non-baseload part. The offshore wind power share drops from approximately 23 billion Euro to zero. Overall, down sampling time series leads to reduced cost and a significantly different capacity mix. Setting this capacity mix as lower bound to the highly resolved model causes large additional costs, mainly because the model deploys much more solar PV than it would otherwise deploy. Vice versa, the downscaled model with the additional constraints from the highly resolved model deploys more offshore wind power and battery storage units than it would deploy in the unconstrained case. Overall, this is expressed in a high sensitivity.

However, there is one effect counteracting this phenomenon. This effect appears when the spatial resolution is modified in addition to the temporal resolution. In this case, averaging takes not only part in the temporal dimension but also in the spatial dimension. More precisely, models with a higher spatial resolution experience less averaging on the spatial scale than models with a coarser spatial resolution—assuming that the models' resolutions are in any case below the resolution of the underlying weather data. This potentially leads to higher capacity factors in the highly resolved case. When transmission capacity is sufficiently available and/or the network is sufficiently meshed, higher capacity factors require less generation capacity as the model with lower spatial resolution. Setting these relatively low

capacities as lower bounds to the coarser model does not lead to any additional costs, because the optimal capacities are above these bounds anyhow. The lower bounds are non-binding. Consequently, the sensitivity is determined by the additional cost arising from setting the optimal capacities of the coarser model as lower bounds to the finer resolved model. Apparently, these additional costs are small compared with the costs arising from modifying the temporal resolution. When the spatial resolution is not modified, both differences in the definition of M (Equation 4) are non-zero. This causes the sensitivity between two models of the same spatial but different temporal resolutions, i.e., (N, 1H) and (N, 24H) to be larger as between two models of different spatial and temporal resolutions (N, 1H) and (*M*, 24H).

DISCUSSION

In this study, we introduced a method to study the sensitivity of power system optimization models to different parameter scenarios and model structures. The core of this method is an error measure M originally designed to measure the error in the results of power system expansion studies originating from the potential discrepancies between the assumptions made for the planning process and the experiences made during the operation phase of power system components. Although they might partly be corrected over time, decisions made based on the model results might be suboptimal in case assumptions turn out to be different from what can be observed in the real world. The model derives a solution, which either is more expensive as the "real" optimal solution or which even does not fulfill the constraints under real world conditions. Investments might be "misallocated." Therefore, M can be understood as measuring the misallocation of investments. As an example, we investigated the error originating from an inaccurate definition of the cost of capital of the power generation assets.

In the subsequent section, it has been shown that the original approach can easily be generalized to measure the sensitivity of any linear program to both changes in model parameters and/or modifications of the model structure. In particular, M quantitatively measures the sensitivity of any pair of similar linear programs on a specific set of scenarios for model parameters and/or the model structure and allows to compare with a great(er) number of scenarios. In fact, M fulfills the properties of a distance measure (or metric): it is positive definite

$$\mathrm{M}_{\alpha_j}^{\alpha_i} \geq 0 \qquad \text{(Equation 5)}$$

because $\Gamma_0^{\alpha_i} \leq \Gamma_{\alpha_j}^{\alpha_i}$, symmetric to the order of the scenarios

$$\mathrm{M}_{\alpha_j}^{\alpha_i} = \mathrm{M}_{\alpha_i}^{\alpha_j} \qquad \text{(Equation 6)}$$

and fulfills the triangle inequality

$$\mathrm{M}_{\alpha_j}^{\alpha_i} \leq \mathrm{M}_{\alpha_k}^{\alpha_i} + \mathrm{M}_{\alpha_j}^{\alpha_k}. \qquad \text{(Equation 7)}$$

The identity of indiscernibles

$$\mathrm{M}_{\alpha_j}^{\alpha_i} = 0 \leftrightarrow \alpha_i = \alpha_j^* \qquad \text{(Equation 8)}$$

is fulfilled if a unique solution of the program exists.

In order to compute M, new constraints must be added to the original program. But since these constraints only define a lower bound for the decision variables, which the program tries to minimize, this cannot cause any infeasibilities. A mathematical proof is given in computing the misallocation metric. Nonetheless, adding the

constraints might affect the convergence of the program. This is hard to estimate and probably crystallizes when the approach is applied.

For testing the developed methodology, we used a simplified setup of a European power system model. For instance, we limited the available technologies for electricity generation to OCGT, wind, solar, and hydro power. Other technologies such as nuclear or combined-cycle gas turbines have not been considered. Furthermore, no coupling of the electricity sector to other sectors has been modeled and rather straightforward approaches to reduce the temporal resolution of the model have been applied, although more sophisticated methods exist (see Hoffmann et al.[47] for an overview). The problems of considering storage units in models with low temporal resolution could be addressed by the approaches of Gabrielli et al.[48] and de Guibert et al.,[49] for instance;however, the explanations for the described sensitivities are rather general. We believe that including more technologies and/or incorporating sector coupling would not influence these general findings and the general applicability of the proposed method.

Nevertheless, it seems reasonable to compare and combine the proposed methods with the approach of Nacken et al[36] or the methods to investigate the shape of the solution space proposed by Neumann and Brown[27] to study the uncertainty of energy system models in future research. The sensitivity to modifications in the temporal resolution could be further investigated by applying the approaches of coupling design periods introduced by Gabrielli et al.[48] and Kotzur et al.[50] or the time series aggregation approach based on hierarchical clustering with connectivity published by Pineda and Morales.[51] Furthermore, it is left open to investigate the robustness of M, for instance, to correlated parameters or reductions in the cost of key technologies, the effect of single technologies on the sensitivity of the PSEM, and the behavior of M in multi-stage optimization problems, which allow to adapt the solution over time.

As mentioned earlier, various approaches to address uncertainty and/or sensitivities of PSEM exist. These approaches can be divided into two approaches, which are to (1) assess the uncertainty based on a comparably small number of deterministic scenarios and (2) use a more systematic (statistical) approach.[42] According to Yue et al.,[42] most power system expansion studies investigate the sensitivity of their results following the first approach. Here, the results obtained from a small set of scenarios are compared against a chosen reference. Despite some obvious shortcomings compared with statistical approaches such as Monte-Carlo simulations, MGA, or robust optimization techniques regarding its statistical robustness, this approach has the advantage of being much less computationally expensive. Furthermore, the data needed to derive statistically robust information—as required for Monte-Carlo simulations for instance—are seldom available in sufficient quality and quantity. On the other hand, choosing a reference often appears arbitrary. Usually, there is no measured observation, i.e., no "reality" that the model results could be compared against, but rather a small number of more or less equally probable and plausible scenarios. Our approach can be classified somewhere in between the two groups of approaches to investigate sensitivities in PSEM. On the one hand, it allows for the situation of having only few scenarios and limited computational resources available. On the other hand, it defines a systematic approach and a sensitivity measure, which exhibits clearly defined mathematical properties (those of a metric). Being comparable with the methods applied by Nacken et al[36] and Neumann and Brown[27] in the sense of modifying and re-solving the original optimization problem, M quantifies the sensitivity by a metric instead of exploring

it visually. Furthermore, it can be applied to almost any kind of optimization model. As such, the obstacles for establishing our approach as a standard to disclose sensitivity information in power system research seem to be comparably low.

In particular, the following conclusions can be drawn from our experiments:

(1) For the (few) scenarios of the spatial resolution used in this study, we find a relatively small sensitivity to increases and decreases in the number of nodes. As long as the temporal resolution of the underlying time series does not include any information about microscale meteorological processes (which hourly time series usually do not), modeling the European power system with only a few dozens of nodes seems reasonable. This may change when more detailed information about the regional distribution of the demand and demand-side flexibilities are included.
(2) In contrast, the temporal resolution of the underlying time series must be chosen carefully, especially with storage devices involved. The power system model shows the highest sensitivity to modifications of the temporal resolution across the characteristic storage horizon of the storage devices. As a conclusion, the temporal resolution should be chosen such that the variability, which the storage devices are supposed to balance, is well represented. Particularly, a temporal resolution lower than 6-hourly might cause misleading results when daily storage units—such as batteries—are considered. Contrarily, time series with daily resolution might be appropriate when only weekly and/or seasonal storage types are part of the model.
(3) We showed that common PSEM exhibit significant sensitivities, in-line with many other studies in the field. Considering the potential political and societal impacts of power system studies, it appears crucial to quantify and report these model sensitivities and uncertainties along with the model results. Our approach is one possible, easily applicable way to achieve this for a great number of applications, not only PSEMs.

EXPERIMENTAL PROCEDURES

Resource availability

Lead contact

Further information and requests for resources should be directed to and will be fulfilled by the lead contact, Bruno Schyska (bruno.schyska@dlr.de).

Materials availability

This study did not generate new unique materials.

Data and code availability

The code used to generate the results reported in this study will be made available on the gitlab page of DLR, Institute of Networked Energy Systems (https://gitlab.com/dlr-ve).

Power system model and data

In this study, we investigate the sensitivity of a common power system expansion problem to (1) different cost of capital assumptions and (2) different temporal and spatial resolutions. The model is formulated as follows[20,28,52]:

$$\min_{\overline{g},g,\overline{f},f} \quad \sum_{n,s} C_{n,s} \cdot \overline{g}_{n,s} + \sum_{l} C_l \cdot L_l \cdot \overline{f}_l + \sum_{n,s,t} O_{n,s} \cdot g_{n,s,t} \qquad \text{(Equation 9)}$$

$$\text{s. t.} \quad \sum_{s} g_{n,s,t} - D_{n,t} = \sum_{l} K_{n,l} \cdot f_l \qquad \text{(Equation 10)}$$

$$G^{-}_{n,s,t}\overline{g} \leq n, sg_{n,s,t} \leq \tilde{G}_{n,s,t} \cdot \overline{g}_{n,s} \quad , \forall n, t \qquad \text{(Equation 11)}$$

$$\text{soc}_{n,s,t} = \left(1 - \eta^{l}_{n,s}\right) \cdot \text{soc}_{n,s,t-1} + \eta^{u}_{n,s}\text{uptake}_{n,s,t} \quad , \forall n, s, t>1 \qquad \text{(Equation 12)}$$

$$\text{soc}_{n,s,0} = \text{soc}_{n,s,|t|} \quad , \forall n, s \qquad \text{(Equation 13)}$$

$$0 \leq \text{soc}_{n,s,t} \leq \tau_{n,s} \cdot \overline{g}_{n,s} \qquad \text{(Equation 14)}$$

$$|f_l(t)| \leq \overline{f}_l \quad , \forall l \qquad \text{(Equation 15)}$$

$$\sum_{l} \overline{f}_l \cdot L_l \leq \text{CAP}_F \qquad \text{(Equation 16)}$$

$$\sum_{n,s,t} \frac{1}{\eta_{n,s}} \cdot g_{n,s,t} \cdot e_{n,s} \leq \text{CAP}_{\text{CO}_2} \qquad \text{(Equation 17)}$$

$$\overline{g}_{n,s,t}, g_{n,s}, \overline{f}_l, \text{soc}_{n,s,t} \geq 0 \qquad \text{(Equation 18)}$$

The used symbols are explained in Table S1. Constraint (Equation 10) ensures that the generation meets the demand. Constraints (Equations 11, 12, 13, 14, and 15) define the bounds for dispatch and transmission. Here, the potential generation $\overline{g}_{n,s}(t)$ describes the resource availability in case of fluctuating renewable generation facilities. Constraints Equation 12 and Equation 13 ensure the consistency of the state of charge as well as the cyclic use of storage units, where in Equation 12, $uptake_{n,s,t}$ refers to the net energy uptake of the storage unit given as follows:

$$\text{uptake}_{n,s,t} = \eta_1 \cdot g_{n,s,t,\text{store}} - \eta_2^{-1} \cdot g_{n,s,t,\text{dispatch}} + \text{inflow}_{n,s,t} - \text{spillage}_{n,s,t}$$

Upper bounds for system-wide transmission capacities and CO_2 emissions are defined in Equations 16 and 17, respectively. For this paper, no global limit for the net transfer capacities is assumed. In-line with European emission reduction targets, CO_2 emissions are limited to 5% of the historic level of 1990. Upper limits of generation capacities have been derived by restricting the available area to agricultural areas and forest and semi natural areas given in the CORINE Land Cover dataset[53] and by excluding all nature reserves and restricted areas.[54] From the available area, the maximally extendable generation capacity has been computed via fixed densities of 3 MW per square kilometer for onshore wind and 1.45 MW per square kilometer for solar PV, respectively.[44]

Capacity factor time series are commonly derived from reanalysis datasets.[55] In PyPSA-Eur, time series for wind power capacity factors and the inflow to hydroelectric power plants are derived based on the ERA5 reanalysis.[56] Onshore and offshore wind power capacity factors have been computed using the power curves of a 3 MW Vestas V112 with 80 m hub height and the NREL Reference Turbine with 5 MW at 90 m hub height, respectively. Solar PV capacity factor time series have been computed from the Heliosat (SARAH) surface radiation dataset[57] using the electric model of Huld et al.[58] and the electrical parameters of the crystalline silicon panel fitted in the same publication. All solar panels are assumed to face south at a tilting angle of 35 degrees. Hourly electricity demand for all European countries has been obtained from the European Network of Transmission System Operators

Figure 9. Network topology
Topology of the PyPSA-Eur network in its 128-node setup.

(ENTSO-E)[59] and assigned to substations via a linear regression of the GDP and the population. For further details on the dataset and the underlying methodology please see Hörsch and Brown.[45]

From this dataset, the parameters for the corresponding PSEM (9)–(17) have been defined. Therefore, we fixed the nominal power of all hydro power plants and pumped hydro storage units to the values reported by Kies et al.,[60] whereas the nominal power of wind, solar PV, and OCGT power plants can be expanded within given bounds. Additionally, we consider two generic storage types with fixed power-to-energy ratio r:

(1) batteries: $r = 6$ h
(2) hydrogen storage: $r = 168$ h

Their nominal power can be expanded as well. For each technology, the investment and operational costs depicted in Table S2 have been used.

The topology of the network clustered to 128 nodes is shown in Figure 9. The time series aggregation method described in reducing the spatial and temporal resolution of the model is then applied to these clustered networks. Although most PSEM aim at finding optimal solutions for power system design, they may significantly vary in structure and in scope. For a list of models, see, for instance, the Open Energy Platform (https://openenergy-platform.org/factsheets/models/).

Reducing the spatial and temporal resolution of the model

In general, two types of time series aggregation methods can be distinguished. The first one aims at decreasing the number of time steps by reducing the resolution of the parameter time series. The *down sampling* approach described below, for instance, can be assigned to this class.

The second class aims at decreasing the number of time steps, whereas keeping the temporal resolution unchanged. In this way, as much of the temporal variability as

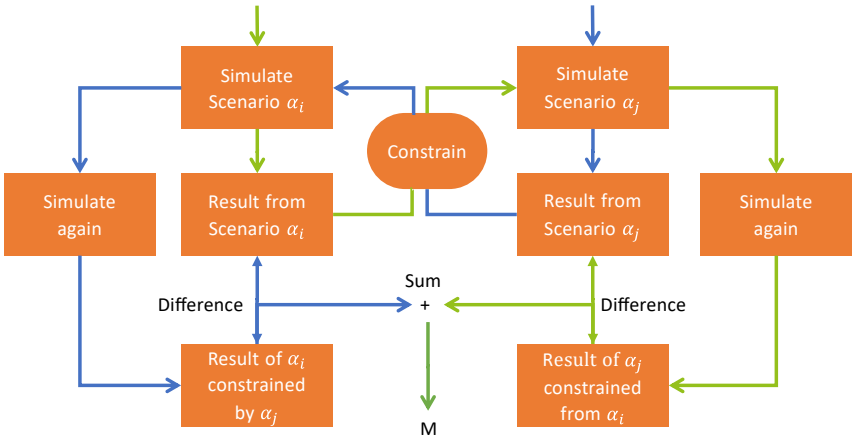

Figure 10. Computing the misallocation metric *M*

The sensitivity of a linear program to two different scenarios for model parameters and/or the model structure can be quantified by constraining both optimizations with the results of the respective other program.

possible shall be conserved. Usually, this is achieved by selecting a limited number of representative *design periods* from the original time series. Depending on the periods' lengths, the variability on different temporal scales can be retained. This, of course, breaks the natural order of the time steps and, consequently, no variability on timescales longer than the periods' lengths can be pictured. Hence, ways need to be found, which allow to model the variability on long timescales (months-seasons), which is represented by the natural inflow into hydro power plants or the seasonal cycle in electricity demand. For an overview of these methodologies, see Pfenninger[25] and Kotzur et al.[61]

In order to account for different time step intervals, weightings need to be defined for each time step considered in the expansion problem: first, in the objective (w_t in Equation 9), and second, in the definition of the storage units' state of charge (ω_t in Equation 12).

For this study, we applied a simple down sampling technique. It averages the original exogenous parameter time series over consecutive time spans of length τ. Hence, it yields $\frac{T}{\tau}$ time steps at constant intervals. The snapshot weightings w_t and ω_t are set to τ.

The spatial resolution of the PSEM is modified by applying the network clustering approach introduced by Hörsch and Brown.[45] The original model is clustered to 45, 64, 90, and 128 nodes.

Computing the misallocation metric

For each of the scenarios α_i the model (9)–(17) is first solved without any lower bounds to the nominal power. In this paper, the additional constraints (Equation 3) are applied to variables representing long-term investment decisions, i.e., generation, storage, and transmission capacities. Meaning, the resulting solution vector for the cost-optimal capacities $[\overline{g}^*_{n,s}]_0^{\alpha_i}$ is then set as the lower bound to the nominal power for the respective partner problem α_j (Figure 10):

$$\left[\overline{g}_{n,s}\right]_{\alpha_i}^{\alpha_j} \geq \left[\overline{g}^*_{n,s}\right]_0^{\alpha_i} \qquad \text{(Equation 19)}$$

Following this procedure in both directions delivers the terms of Equation 4. For this study, constraints (Equation 19) have been applied to all generation and storage assets. The resulting linear programs have been solved using the Python for Power System Analysis tool (PyPSA)[62] and the numerical solver *Gurobi* on the high-performance cluster infrastructure of the German Aerospace Center (DLR) in Oldenburg, Germany.

As mentioned earlier, invoking constraints (Equation 19) should not cause the optimization model to become infeasible. This can be proven as follows: let us assume the original problem is feasible, and let $\{[g^*_{n,s,t}]_0^{\alpha_i}, [\overline{g}^*_{n,s}]_0^{\alpha_i}, [f^*_{l,t}]_0^{\alpha_i}, [\overline{f}^*_{l}]_0^{\alpha_i}\}$ be the solution of the original problem under scenario α_i. We now assume

$$\left[\overline{g}^*_{n,s}\right]_{\alpha_j}^{\alpha_i} = \max\left\{\left[\overline{g}^*_{n,s}\right]_0^{\alpha_i}, \left[\overline{g}^*_{n,s}\right]_0^{\alpha_j}\right\} \quad \text{(Equation 20)}$$

Then

$$\begin{aligned} G^-_{n,s,t}\left[\overline{g}^*_{n,s}\right]_{\alpha_j}^{\alpha_i} &\le G^-_{n,s,t}\left[\overline{g}^*_{n,s}\right]_0^{\alpha_i} \\ &\le g_{n,s,t} \\ &\le \tilde{G}n,s,t\left[\overline{g}^*_{n,s}\right]_0^{\alpha_i} \\ &\le \tilde{G}n,s,t\left[\overline{g}^*_{n,s}\right]_{\alpha_j}^{\alpha_i}, \forall n,t \end{aligned} \quad \text{(Equation 21)}$$

if $G^-_{n,s,t} \le 0$ and $\tilde{G}_{n,s,t} \ge 0$, which it is, in all cases considered here. Consequently, $\{[g^*_{n,s,t}]_0^{\alpha_i}, [\overline{g}^*_{n,s}]_{\alpha_j}^{\alpha_i}, [f^*_{l,t}]_0^{\alpha_i}, [\overline{f}^*_{lf}]_0^{\alpha_i}\}$ is in the feasible space of the new problem, and the problem therefore is not infeasible.

In case the number of substations of the two parameter sets differs, i.e., $N_i \neq N_j$, the lower bounds for each parameter set are computed from the corresponding cluster of buses of the other parameter set: let $\mathcal{N}_i = \{S_{i,1}, S_{i,2}, \ldots, S_{i,m}, \ldots, S_{i,N_i}\}$, $\mathcal{N}_j = \{S_{j,1}, S_{j,2}, \ldots, S_{j,k}, \ldots, S_{j,N_j}\}$ be the two sets of clusters of buses derived from the original full-resolution dataset with $|\mathcal{N}_{i/j}| = N_{i/j}$. In the clustered networks, each of these clusters S is merged into one single bus $n(S_{i,m})$, $n(S_{j,k})$. Then, the lower bound to a generator of technology s at a bus of set $\mathcal{N}_i$ is set to the weighted sum of the optimal capacity of the buses of set $\mathcal{N}_j$ and vice versa:

$$\left[\overline{g}^{min}_{n(S_{i,m}),s}\right]_{\alpha_i}^{\alpha_j} = \sum_{k=1}^{N_j} w_k \left[\overline{g}^*_{n(S_{j,k}),s}\right]_0^{\alpha_i}, \forall S_{i,m}, n(S_{i,m}) \quad \text{(Equation 22)}$$

where the weights w_k are determined from the number of common nodes of the two clusters $S_{i,m}$, $S_{j,k}$:

$$w_k = \frac{|S_{i,m} \cap S_{j,k}|}{|S_{j,k}|} \quad \text{(Equation 23)}$$

Here, $|S_{i,m} \cap S_{j,k}|$ is the number of nodes, which appears in both clusters, i.e., the clusters' intersection.

SUPPLEMENTAL INFORMATION

Supplemental information can be found online at https://doi.org/10.1016/j.joule.2021.07.017.

ACKNOWLEDGMENTS

M.S. and A.K. are financially supported by the research project CoNDyNet II (Bundesministerium für Bildung und Forschung, Fkz. 03EK3055C). The authors thank Jakub Jurasz for helping with Figures 1, 2, and 4 as well as four anonymous reviewers for their thorough reviews and helpful comments.

AUTHOR CONTRIBUTIONS

Conceptualization, B.U.S. and A.K.; methodology, B.U.S. and A.K.; investigation, B.U.S.; writing and original draft preparation, B.U.S. and A.K.; resources, M.S.; project administration and funding acquisition, all authors; writing – review and editing, L.v.B. and W.M.

DECLARATION OF INTERESTS

The authors declare no competing interests.

Received: March 10, 2021
Revised: June 18, 2021
Accepted: July 29, 2021
Published: August 24, 2021

REFERENCES

1. Pacala, S., and Socolow, R. (2004). Stabilization wedges: solving the climate problem for the next 50 years with current technologies. Science *305*, 968–972.
2. Lund, H. (2007). Renewable energy strategies for sustainable development. Energy *32*, 912–919.
3. Connolly, D., Lund, H., Mathiesen, B.V., and Leahy, M. (2010). A review of computer tools for analysing the integration of renewable energy into various energy systems. Appl. Energy *87*, 1059–1082.
4. Steinke, F., Wolfrum, P., and Hoffmann, C. (2013). Grid vs. storage in a 100% renewable Europe. Renew. Energy *50*, 826–832.
5. Weitemeyer, S., Kleinhans, D., Wienholt, L., Vogt, T., and Agert, C. (2016). A European perspective: potential of grid and storage for balancing renewable power systems. Energy Technol. *4*, 114–122.
6. Rodríguez, R.A., Becker, S., Andresen, G.B., Heide, D., and Greiner, M. (2014). Transmission needs across a fully renewable European power system. Renew. Energy *63*, 467–476.
7. Kies, A., Schyska, B.U., and von Bremen, L. (2016a). Curtailment in a highly renewable power system and its effect on capacity factors. Energies *9*, 510.
8. Heide, D., Greiner, M., Von Bremen, L., and Hoffmann, C. (2011). Reduced storage and balancing needs in a fully renewable European power system with excess wind and solar power generation. Renew. Energy *36*, 2515–2523.
9. Grams, C.M., Beerli, R., Pfenninger, S., Staffell, I., and Wernli, H. (2017). Balancing Europe's wind power output through spatial deployment informed by weather regimes. Nat. Clim. Chang. *7*, 557–562.
10. Ming, B., Liu, P., Guo, S., Zhang, X., Feng, M., and Wang, X. (2017). Optimizing utility-scale photovoltaic power generation for integration into a hydropower reservoir by incorporating long- and short-term operational decisions. Appl. Energy *204*, 432–445.
11. Jurasz, J., and Ciapała, B. (2017). Integrating photovoltaics into energy systems by using a run-off-river power plant with pondage to smooth energy exchange with the power grid. Appl. Energy *198*, 21–35.
12. Santos-Alamillos, F.J., Pozo-Vázquez, D., Ruiz-Arias, J.A., Von Bremen, L., and Tovar-Pescador, J. (2015). Combining wind farms with concentrating solar plants to provide stable renewable power. Renew. Energy *76*, 539–550.
13. Sepulveda, N.A., Jenkins, J.D., de Sisternes, F.J., and Lester, R.K. (2018). The role of firm low-carbon electricity resources in deep decarbonization of power generation. Joule *2*, 2403–2420.
14. Brown, P.R., and Botterud, A. (2021). The value of inter-regional coordination and transmission in decarbonizing the us electricity system. Joule *5*, 115–134.
15. Kies, A., Schyska, B.U., and von Bremen, L. (2016b). The demand side management potential to balance a highly renewable European power system. Energies *9*, 955.
16. Hirth, L., and Müller, S. (2016). System-friendly wind power. Energy Econ *56*, 51–63.
17. Chattopadhyay, K., Kies, A., Lorenz, E., von Bremen, L., and Heinemann, D. (2017). The impact of different pv module configurations on storage and additional balancing needs for a fully renewable European power system. Renew. Energy *113*, 176–189.
18. Pfenninger, S., Gauché, P., Lilliestam, J., Damerau, K., Wagner, F., and Patt, A. (2014). Potential for concentrating solar power to provide baseload and dispatchable power. Nature Clim. Change *4*, 689–692.
19. Lund, H., and Kempton, W. (2008). Integration of renewable energy into the transport and electricity sectors through v2g. Energy Policy *36*, 3578–3587.
20. Brown, T., Schlachtberger, D., Kies, A., Schramm, S., and Greiner, M. (2018a). Synergies of sector coupling and transmission reinforcement in a cost-optimised, highly renewable European energy system. Energy *160*, 720–739.
21. Spencer, T., Rodrigues, N., Pachouri, R., Thakre, S., and Renjith, G. (2020). Renewable power pathways: modelling the integration of wind and solar in India by 2030 (Teri the Energy and Resources Institute). https://www.teriin.org/sites/default/files/2020-07/Renewable-Power-Pathways-Report.pdf.
22. Pescia, D. (2020). Minimizing the Cost of Integrating Wind and Solar Power in Japan. Insights for Japanese power system transformation up to 2030. ANALYSIS (Agora Energiewende).
23. Lotze, J., Salzinger, M., Gaillardon, B., Mogel, M., and Troitskyi, K. (2020). Stromnetz 2050, Technical report (TransnetBW), Stuttgart. https://www.transnetbw.de/de/stromnetz2050/.
24. Pfenninger, S. (2017a). Energy scientists must show their workings. Nature *542*, 393.
25. Pfenninger, S. (2017b). Dealing with multiple decades of hourly wind and pv time series in energy models: a comparison of methods to reduce time resolution and the planning implications of inter-annual variability. Appl. Energy *197*, 1–13.

26. Hilbers, A.P., Brayshaw, D.J., and Gandy, A. (2019). Quantifying demand and weather uncertainty in power system models using the m out of n bootstrap. arXiv, arXiv:1912.10326.

27. Neumann, F., and Brown, T. (2019). The near-optimal feasible space of a renewable power system model. arXiv, arXiv:1910.01891.

28. Schlott, M., Kies, A., Brown, T., Schramm, S., and Greiner, M. (2018). The impact of climate change on a cost-optimal highly renewable European electricity network. Appl. Energy *230*, 1645–1659.

29. Schyska, B.U., and Kies, A. (2020). How regional differences in cost of capital influence the optimal design of power systems. Appl. Energy *262*, 114523.

30. Frysztacki, M.M., Hörsch, J., Hagenmeyer, V., and Brown, T. (2021). The strong effect of network resolution on electricity system models with high shares of wind and solar. Appl. Energy *291*, 116726.

31. Trutnevyte, E. (2016). Does cost optimization approximate the real-world energy transition? Energy *106*, 182–193.

32. Mavromatidis, G., Orehounig, K., and Carmeliet, J. (2018). Uncertainty and global sensitivity analysis for the optimal design of distributed energy systems. Appl. Energy *214*, 219–238.

33. Schlachtberger, D.P., Brown, T., Schäfer, M., Schramm, S., and Greiner, M. (2018). Cost optimal scenarios of a future highly renewable European electricity system: exploring the influence of weather data, cost parameters and policy constraints. Energy *163*, 100–114.

34. Moret, S., Codina Gironès, V.C., Bierlaire, M., and Maréchal, F. (2017). Characterization of input uncertainties in strategic energy planning models. Appl. Energy *202*, 597–617. https://doi.org/10.1016/j.apenergy.2017.05.106.

35. Shirizadeh, B., Perrier, Q., and Quirion, P. (2019). How sensitive are optimal fully renewable power systems to technology cost uncertainty? Policy Papers 2019.04 (FAERE - French Association of Environmental and Resource Economists). https://ideas.repec.org/p/fae/ppaper/2019.04.html.

36. Nacken, L., Krebs, F., Fischer, T., and Hoffmanna, C. (2019). Integrated renewable energy systems for Germany–a model-based exploration of the decision space. In 2019 16th International Conference on the European Energy Market (EEM), pp. 1–8.

37. Brill, E.D., Jr., Chang, S.-Y., and Hopkins, L.D. (1982). Modeling to generate alternatives: the hsj approach and an illustration using a problem in land use planning. Manag. Sci. *28*, 221–235.

38. Price, J., and Keppo, I. (2017). Modelling to generate alternatives: a technique to explore uncertainty in energy-environment-economy models. Appl. Energy *195*, 356–369.

39. DeCarolis, J.F., Babaee, S., Li, B., and Kanungo, S. (2016). Modelling to generate alternatives with an energy system optimization model. Environ. Modell. Software *79*, 300–310.

40. Louwen, A., Junginger, M., and Krishnan, S. (2018). Technological learning in energy modelling–experience curves: policy brief for the reflex project. https://reflex-project.eu/wp-content/uploads/2018/12/REFLEX_policy_brief_Experience_curves_12_2018.pdf.

41. Mattsson, N., and Wene, C.-O. (1997). Assessing new energy technologies using an energy system model with endogenized experience curves. Int. J. Energy Res. *21*, 385–393.

42. Yue, X., Pye, S., DeCarolis, J., Li, F.G.N., Rogan, F., and Gallachóir, B.Ó. (2018). A review of approaches to uncertainty assessment in energy system optimization models. Energy Strategy Rev *21*, 204–217. https://doi.org/10.1016/j.esr.2018.06.003.

43. Noothout, P., de Jager, D., Tesnière, L., van Rooijen, S., Karypidis, N., Brückmann, R., Jirouš, F., Breitschopf, B., Angelopoulos, D., Doukas, H., et al. (2016). The impact of risks in renewable energy investments and the role of smart policies (Diacore). http://www.indiaenvironmentportal.org.in/files/file/impact-of-risk-in-res-investments.pdf.

44. Hörsch, J., Hofmann, F., Schlachtberger, D., and Brown, T. (2018). Pypsa-eur: an open optimisation model of the European transmission system. arXiv, arXiv:1806.01613.

45. Hörsch, J., and Brown, T. (2017). The role of spatial scale in joint optimisations of generation and transmission for European highly renewable scenarios. In 2017 14th International Conference on the European Energy Market (EEM), pp. 1–7.

46. St. Martin, C.M.S., Lundquist, J.K., and Handschy, M.A. (2015). Variability of interconnected wind plants: correlation length and its dependence on variability time scale. Environ. Res. Lett. *10*, 044004.

47. Hoffmann, M., Kotzur, L., Stolten, D., and Robinius, M. (2020). A review on time series aggregation methods for energy system models. Energies *13*, 641.

48. Gabrielli, P., Gazzani, M., Martelli, E., and Mazzotti, M. (2018). Optimal design of multi-energy systems with seasonal storage. Appl. Energy *219*, 408–424.

49. de Guibert, P., Shirizadeh, B., and Quirion, P. (2020). Variable time-step: a method for improving computational tractability for energy system models with long-term storage. Energy *213*, 119024.

50. Kotzur, L., Markewitz, P., Robinius, M., and Stolten, D. (2018a). Time series aggregation for energy system design: modeling seasonal storage. Appl. Energy *213*, 123–135.

51. Pineda, S., and Morales, J.M. (2018). Chronological time-period clustering for optimal capacity expansion planning with storage. IEEE Trans. Power Syst. *33*, 7162–7170.

52. Schlachtberger, D.P., Brown, T., Schramm, S., and Greiner, M. (2017). The benefits of cooperation in a highly renewable European electricity network. Energy *134*, 469–481.

53. Copernicus Programme. (2017). Corine land cover. https://land.copernicus.eu/pan-european/corine-land-cover/clc-2012.

54. European Environment Agency (2016). Natura 2000 data, the European network of protected sites. https://www.eea.europa.eu/data-and-maps/data/natura-7.

55. Jurasz, J., Canales, F.A., Kies, A., Guezgouz, M., and Beluco, A. (2020). A review on the complementarity of renewable energy sources: concept, metrics, application and future research directions. Sol. Energy *195*, 703–724.

56. Copernicus Climate Change Service (2017). Era5: Fifth generation of ecmwf atmospheric reanalyses of the global climate (Copernicus), Copernicus Climate Change Service Climate Data Store (CDS). https://www.ecmwf.int/en/forecasts/dataset/ecmwf-reanalysis-v5.

57. Pfeifroth, U., Kothe, S., Müller, R., Trentmann, J., Hollmann, R., Fuchs, P., and Werscheck, M. (2017). Surface radiation data set - heliosat (sarah) - edition 2.1. Technical report, Satellite Application Facility on Climate Monitoring (CM-SAF). https://doi.org/10.5676/EUM_SAF_CM/SARAH/V002_01.

58. Huld, T., Gottschalg, R., Beyer, H.G., and Topič, M. (2010). Mapping the performance of pv modules, effects of module type and data averaging. Sol. Energy *84*, 324–338.

59. ENTSO-E. (2012). Country-specific hourly load data. https://www.entsoe.eu/data/data-portal/.

60. Bremen, L.V., Buddeke, M., Heinemann, D., Kies, A., Kleinhans, D., Krüger, C., et al. (2021). Ergebnisse und Empfehlungen des BMBF-Forschungsprojektes Regenerative Stromversorgung & Speicherbedarf in 2050-RESTORE 2050: Teilbericht D13+ D14., Technical report (Wuppertal Institut). https://epub.wupperinst.org/files/7786/7786_RESTORE2050.pdf.

61. Kotzur, L., Markewitz, P., Robinius, M., and Stolten, D. (2018b). Impact of different time series aggregation methods on optimal energy system design. Renew. Energy *117*, 474–487.

62. Brown, T., Hörsch, J., and Schlachtberger, D. (2018b). PyPSA: Python for Power System Analysis. J. Open Res. Software *6*. https://doi.org/10.5334/jors.188.